Post-Earthquake Assessment of an Educational Masonry Building After the 2019 Albania Earthquake

Marjo Hysenlliu,[1] Altin Bidaj,[1] Huseyin Bilgin[2*]

[1]Department of Civil Engineering, Faculty of Civil Engineering, Polytechnic University of Tirana, Tirana, Albania
[2]Department of Civil Engineering, Faculty of Architecture and Engineering, EPOKA University, Tirana, Albania
*hbilgin@epoka.edu.al

Abstract

Albania and the broader region possess a considerable inventory of low- and mid-rise unreinforced masonry buildings dating from the post-World War II era till 1990s. Many structures of this type have shown vulnerability in recent seismic events in the region and succumbed to destruction during the catastrophic 2019 Albania earthquake sequences, resulting in loss of life, injuries, and property damage. The structures in question typically range from three to five stories in height and feature clay brick masonry walls, along with rigid floor slabs. This study outlines a case study focusing on a URM school building that sustained damage during the 2019 Albania earthquake. Geotechnical investigations were carried out to characterize the soil conditions at the sites of the school foundations. Nonlinear static analyses were conducted to evaluate the seismic capacity, determine the performance point, and define damage states, based on a performance-based assessment methodology. The analysis of capacity curves and performance metrics revealed significant structural deficiencies in the school buildings. Findings indicate that buildings constructed before the adoption of modern seismic codes do not meet current performance criteria, underscoring the need for immediate strengthening measures and risk mitigation strategies.

Keywords

unreinforced masonry (URM), seismic vulnerability assessment, equivalent frame method (EFM), non-linear static pushover analysis, Eurocode 8 performance limits, structural retrofitting

Research article

2026 | Vol. 1 | e001

DOI

Received: 22 December 2025 | **Revised:** 25 February 2026; 20 March 2026 | **Accepted:** 21 March 2026 | **Published:** 21 April 2026

How to cite: Hysenlliu M, Bidaj A, Bilgin H. Post-Earthquake Assessment of an Educational Masonry Building After the 2019 Albania Earthquake. Resilience and Reuse in the Built Environment. 2026; 1:e001.

Introduction

A comprehensive understanding of a region's seismic history is fundamental to evaluating the likelihood of future earthquake occurrences and estimating the potential severity of their impacts. The extent of expected damage is primarily governed by the vulnerability of the built environment; however, historical seismicity serves as a key indicator of the underlying hazard, particularly in tectonically active areas with documented earthquake events.

Albania is located in a seismically active zone at the convergence of the African and Eurasian tectonic plates, which has long subjected the region to frequent and sometimes devastating earthquakes. This seismic vulnerability was tragically highlighted by the 2019 Albania earthquake, which struck the Durrës region with a moment magnitude (Mw) of 6.4, causing widespread destruction, loss of life, and significant socio-economic disruption. Statistical records and historical data reveal that Albania and the broader Southwestern Balkans experience moderate to strong earthquakes (Mw 5.5–6.9) at irregular but recurring intervals, with major seismic events historically impacting densely populated areas along the Adriatic coast and inland fault zones. Albania's seismic hazard is primarily shaped by a complex system of active faults, including the Shkoder–Peja, Elbasan–Dibra, and Vlora–Korça fault zones, which reflect the region's existing compressional tectonic regime. The 2019 earthquake highlighted the critical need for enhanced seismic risk reduction and improved building resilience measures within the country, while also drawing attention to the wider regional risks associated with active tectonics across the Balkans and Eastern Mediterranean countries.

Historically, earthquakes in Albania—similar to those in other seismically active countries—have inflicted severe damage on buildings, leading to substantial human casualties and economic losses, as documented by several researchers [1-4]. In this context, the concept of structural vulnerability becomes central to efforts aimed at mitigating the impacts of such catastrophic events. Among various building typologies, unreinforced masonry structures generally perform worse under seismic loading with respect to RC buildings, mainly due to their low inherent strength, stiffness, and ductility. Modern seismic design codes have introduced new provisions to mitigate the vulnerability of masonry buildings. However, a considerable part of the existing masonry building stock predates these modern standards and was often built according to old codes.

Albania's building stock is largely comprised of unreinforced URM structures with load-bearing masonry walls, as well as RC frame buildings featuring infill walls made of red/silicate clay bricks or concrete blocks. Mixed structural systems are also commonly found. Most of these buildings were designed and constructed following the Albanian Technical Codes (KTPs), first issued in 1963 and later updated in 1989. These codes are still legally valid and remain in use today. Similar to many European countries, Albania's existing masonry structures were often designed under earlier seismic regulations, specifically KTP-63 and KTP-N2 (1989), which either omitted seismic design requirements or focused on reducing seismic forces rather than ensuring structural resilience. As a result, the seismic provisions in these codes are considerably less rigorous than those mandated by contemporary standards such as EC-6 and EC-8. This has led to insufficient seismic considerations in the design of many buildings across the country. Although the European Norms (EN) versions of the Eurocodes have been adopted in recent years for the design of new structures, and several companies and engineering firms have begun incorporating them into their practices, Albanian legislation still mandates the use of KTPs for official structural design. As noted by Bilgin and Frangu (2017) [5], the Eurocodes are recognised as national standards, but their application remains voluntary within the current legal framework.

The URM buildings were highly affected by the November 26, 2019, Durrës Earthquake. Contributing factors included the age of the buildings, poor construction quality, substandard workmanship, unauthorised modifications, outdated design codes, lack of protection, and insufficient repairs following previous tremors.

The focus of this study is a primary school block, located in the Albanian capital, Tirana, which also sustained significant destruction during the Durrës Earthquake sequences. School structures play a key function in each society, and maintaining their functionality after natural disasters is essential. In

seismically active regions, these structures must be designed to resist earthquakes, as their failure can significantly disrupt community life and interrupt educational activities. Recent destructive tremors in Albania, Algeria, Greece, India, Iran, Italy, Morocco, and Turkey have exposed the insufficient seismic resilience of many school facilities, as reported in studies [6-8]. During site inspections, the overall state of the buildings was assessed, including observable ground settlements and cracks in the structure. Damage assessments were then compiled based on data obtained from the original blueprints and site visits to the buildings.

This paper aims to assess the earthquake response of template low-rise URM school structures, constructed according to old practices in Albanian territory. To represent the characteristics of these buildings, two URM school structures with standard designs were chosen and modelled by 3Muri software, following the approach of Lagomarsino et al. [9].

Structural features such as member dimensions, material types, and loading conditions were derived from the architectural and structural design plans, as well as field investigations of similar buildings in various cities across Albania. Material properties were obtained experimentally and applied in the nonlinear analysis. Pushover analyses were conducted to evaluate the seismic response in accordance with EC 8.

Tectonic setting and impacts of the 2019 Albania earthquake sequences

Albania's seismicity is driven by its position within the complex zone of collision between the Adriatic (part of the African plate) and the Eurasian plate. The region is characterised by active thrust faulting and transpressional tectonics, producing significant seismic hazards. Major fault zones in Albania include the Shkodra–Peja fault, the Elbasan–Dibra fault, and the Vlora–Korça fault zone. These systems exhibit moderate to high activity and pose threats to both urban and rural settlements. Historical records indicate recurring destructive earthquakes in central and western Albania. The 2019 Durrës earthquake occurred along a thrust fault offshore of Durrës, where strain accumulation is high due to ongoing crustal compression (Figure 1).

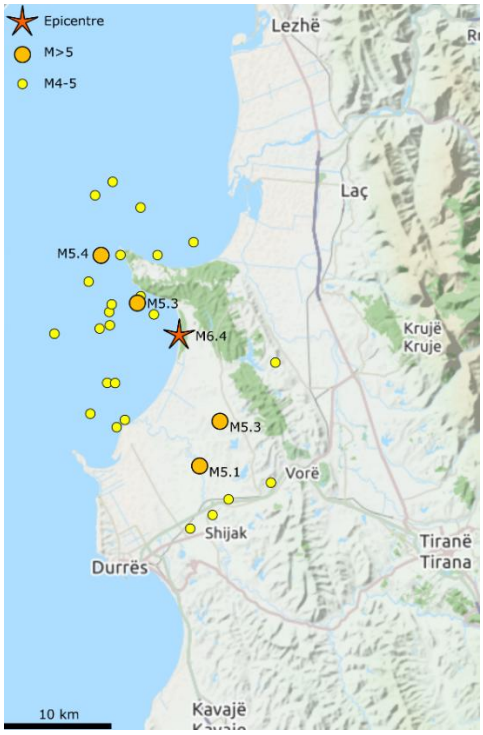

Figure 1. Location of epicentre and important aftershocks of the 2019 Albania earthquakes.

According to the Seismic Zonation Map of Albania (Figure 2a), as outlined in the Seismic Design Regulations issued in 1989 by the Ministry of Construction's Department of Design [10], the observed earthquake intensities fall within the prescribed limits. Additionally, based on the probabilistic approach, the seismic hazard maps for peak ground acceleration with a 475-year recurrence period are presented for hard rock site conditions (Figure 2b).

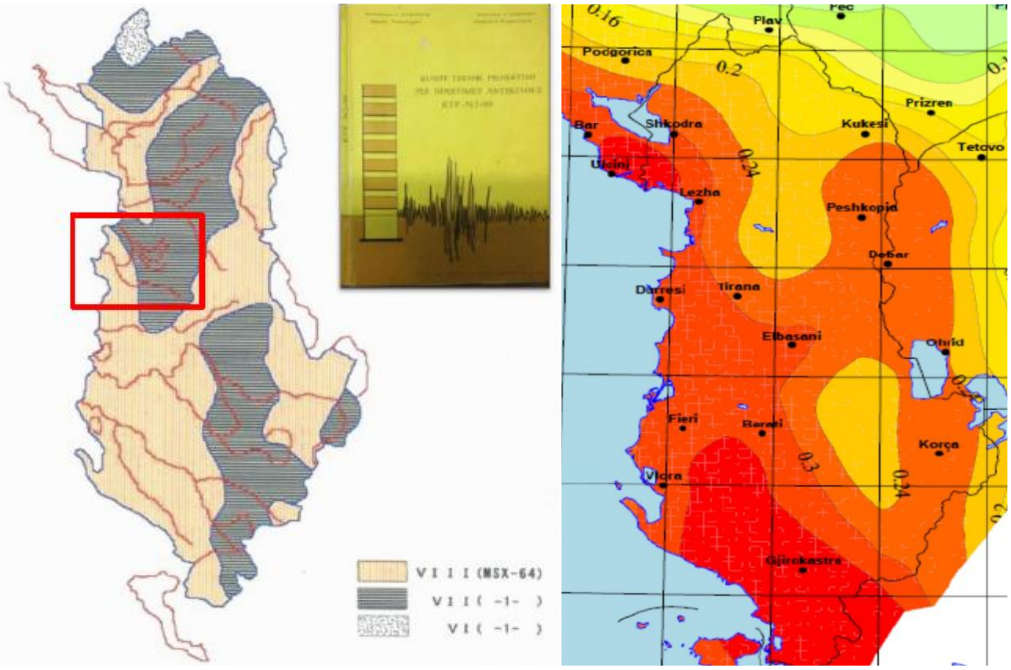

a) b)

Figure 2. a) Earthquake zonation map, b) Probabilistic seismic hazard map for horizontal peak ground acceleration, for 475 years, (hard rock) [11].

Official statistics indicate that Tirana and Durrës together contribute to over one-quarter of the total urban seismic risk. Moreover, Albania's six most at-risk cities collectively represent more than two-thirds of the overall urban seismic risk (Figure 3).

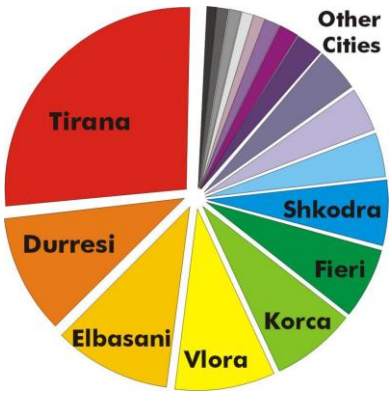

Figure 3. Urban seismic risk in Albanian territory [12].

Observed Damage Patterns

Field surveys following the 2019 earthquake documented extensive damage to unreinforced masonry (URM) residential and public buildings, particularly those constructed before the enforcement of modern seismic codes. Common damage modes included vertical cracks at wall corners, diagonal shear cracks, out-of-plane wall failures, and total collapse of unsupported walls. Several mid-rise reinforced concrete buildings also exhibited soft-story failures due to commercial ground floors with reduced lateral stiffness. Heritage structures such as mosques experienced partial collapses, while schools and hospitals showed varying degrees of damage depending on their age and construction quality.
Building damage was primarily concentrated along two elliptical zones, with their major axes generally oriented in a northwest-southeast (NW-SE) direction. This orientation aligns with the strike of the seismogenic fault, as indicated by fault plane solutions from various seismological institutes and observatories [13-14] (Figure 4).

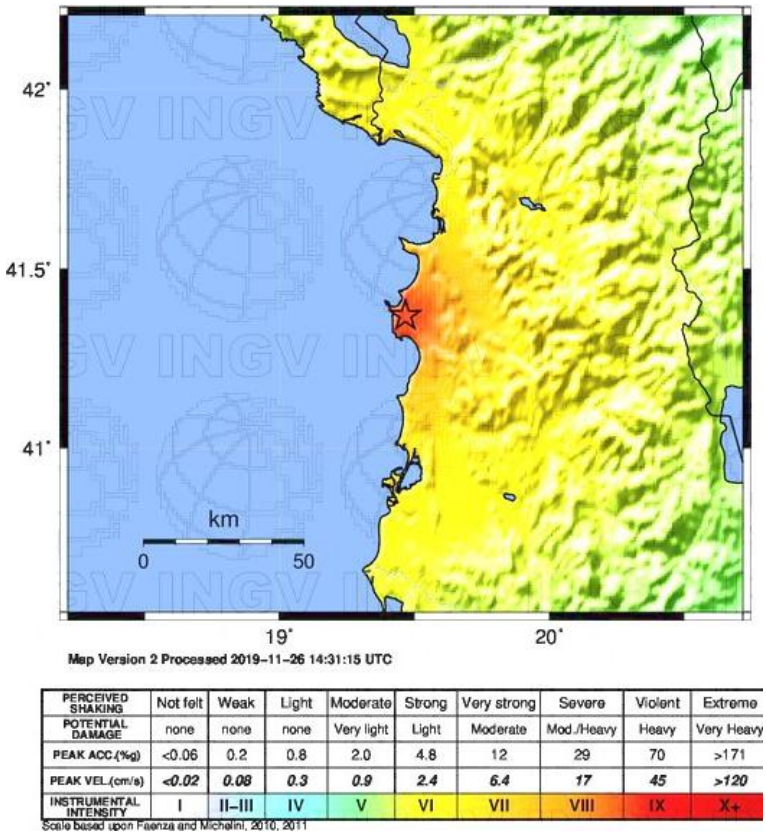

PERCEIVED SHAKING	Not felt	Weak	Light	Moderate	Strong	Very strong	Severe	Violent	Extreme
POTENTIAL DAMAGE	none	none	none	Very light	Light	Moderate	Mod./Heavy	Heavy	Very Heavy
PEAK ACC.(%g)	<0.06	0.2	0.8	2.0	4.8	12	29	70	>171
PEAK VEL.(cm/s)	*<0.02*	*0.08*	*0.3*	*0.9*	*2.4*	*6.4*	*17*	*45*	*>120*
INSTRUMENTAL INTENSITY	I	II–III	IV	V	VI	VII	VIII	IX	X+

Scale based upon Faenza and Michelini, 2010, 2011

Figure 4. Shakemap of the 2019 Albania Earthquake [13].

The extent of the damage is largely due to the proximity of the main fault to the cities of Durrës and Tirana, which resulted in considerable structural damage and partial collapse of numerous buildings. The earthquake impacted both newly constructed and older buildings, underscoring the vulnerability of the region's building stock. Typical failure modes observed in various types of masonry structures are illustrated in Figures 5-7.

a) b)

Figure 5. a) In-plane failure of masonry, b) Lack of proper anchorage.

In many of the damaged structures, in-plane shear failures were frequently seen, often manifested as double-diagonal shear cracks. In numerous older structures across Albania, excessive shear or bending forces led to significant in-plane damage (Figure 5a). In the absence of proper anchorage, exterior walls acted as cantilevers along the height of the buildings, leading to failures in numerous structures (Figure 5b). In masonry facades with numerous window openings, shear failures were frequently observed in spandrels and short piers (Figure 6). Additional damage observed in unreinforced masonry (URM) buildings was attributed to the absence of rigid diaphragm action (Figure 7a). Failures resulting from poor material quality were also prevalent in many masonry buildings (Figure 7b).

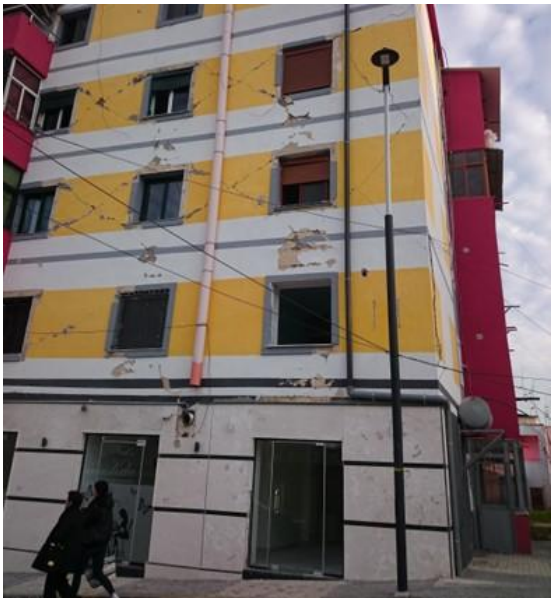

Figure 6. In-plane shear failure of masonry piers.

a) b)

Figure 7. a) Diaphragm-related failures, b) Poor material and substandard workmanship-related failures.

Evaluation of a school building's structural integrity and load-bearing systems' compliance with earthquake-resistant standards

The seismic resilience of school buildings is a critical concern due to their dual function as educational centres and emergency shelters [15-16]. Past earthquake events have underscored the vulnerability of many school buildings, particularly those constructed without modern seismic design standards [1,17]. These structures are vital to community recovery and continuity of education post-disaster, making their performance under seismic loads a top priority [18-19]. Therefore, protection of these structures through robust design practices, regular evaluations, and timely retrofitting can substantially reduce risks to human life and property while enhancing emergency response capabilities [20-21]. Research consistently shows that many school buildings suffer from structural deficiencies due to poor construction materials, ageing, or the absence of adequate seismic design provisions [2,22,23]. Thorough vulnerability assessments, employing both advanced analytical models and rapid visual screening methods, are essential for identifying weaknesses in structural and non-structural components [24-25]. When integrated with probabilistic frameworks, these assessments enable the development of targeted retrofit strategies that prioritise both life safety and post-disaster functionality [18,26]. Moreover, combining engineering insights with socio-economic considerations enhances community preparedness and resilience in the wake of seismic hazards [27].

Modern retrofitting approaches, informed by empirical studies and performance-based earthquake engineering principles, have been shown to significantly enhance the seismic resilience of school buildings [28-29]. Research and practical case studies underscore the importance of upgrading both structural and non-structural elements to ensure that educational facilities remain operational during and after seismic events [20,30]. The adoption of analytical frameworks that integrate GIS technologies, economic considerations, and multi-hazard assessments has increased the effectiveness and precision of retrofit strategies [31-32]. These advanced methodologies support the formulation of region-specific building codes and policies, contributing to more resilient educational infrastructure and urban planning [33-34].

Interdisciplinary collaboration is crucial for enhancing seismic safety within the educational sector. Effective coordination among engineers, urban planners, and policymakers is necessary to ensure that

school buildings comply with modern safety standards and are capable of fulfilling their essential roles in the aftermath of earthquakes [21,26]. Investments in research, retrofitting technologies, and continuous maintenance yield long-term societal benefits by preserving life, reducing economic losses, and sustaining social and civic infrastructure [15,35]. In conclusion, resilient educational infrastructure is not only a technical necessity but also a vital component of disaster preparedness and sustainable community development.

Building Description and As-Built Configuration

The primary unit of analysis is the main three-story URM school block, which houses the primary educational facilities and sustained the most significant damage during the 2019 seismic event. The secondary unit is an adjacent, single-story URM sports hall. Because these structures are separated by an adequate seismic gap, they do not exhibit dynamic pounding effects or load sharing; therefore, they were modelled and analysed as two distinct structures within the 3Muri software environment. The examined school and sports hall are situated in Tirana. An overall view of the buildings is presented in Figure 8. The main building floor information, which is the subject of the inspection, is given in Table 1. In addition, typical views of the school structures are given in Figures 9-10.

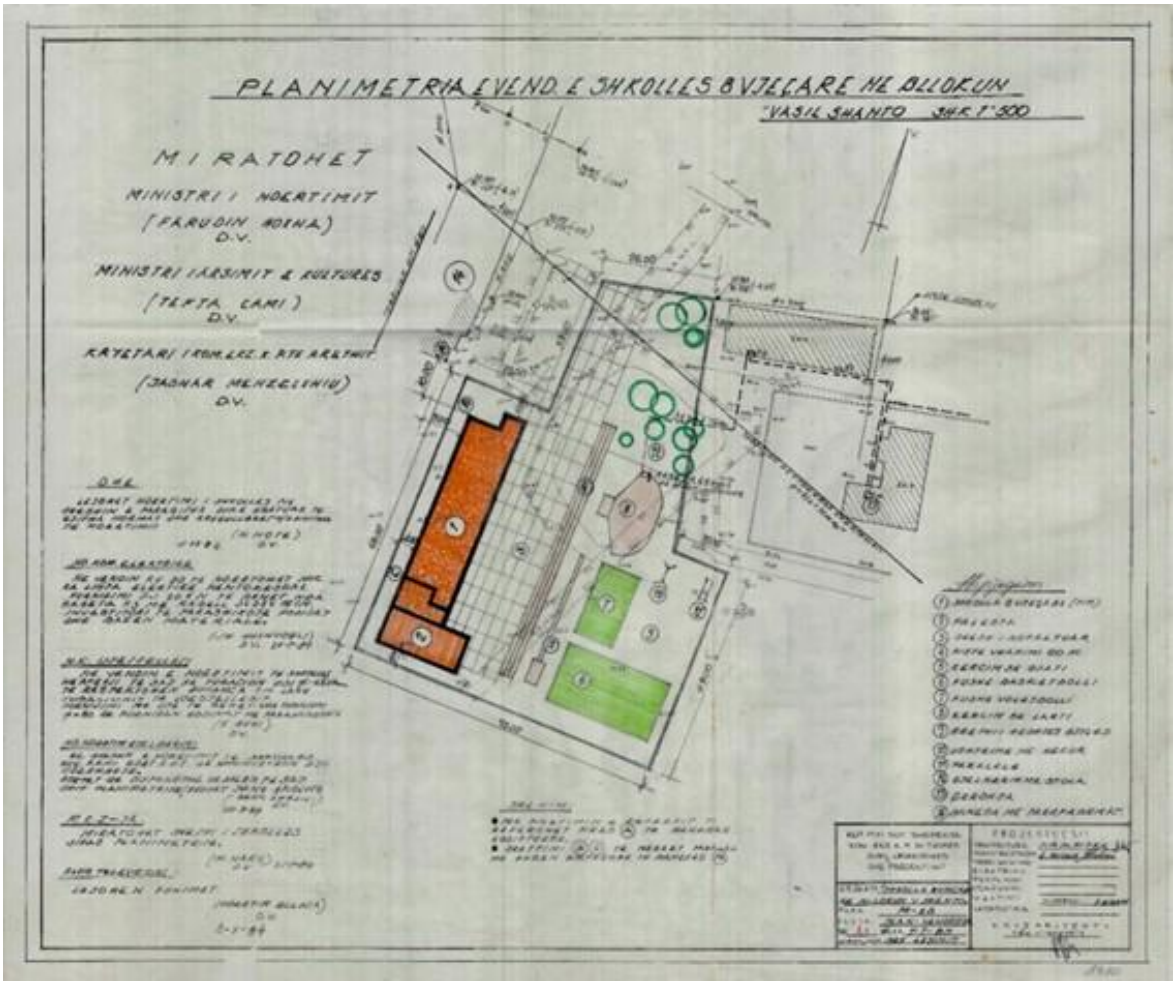

Figure 8. Planimetry of the studied building.

Table 1. Main building and Sport court floor information.

Structural Unit	Number of Stories	Floor Plan Dimensions	Total Area	Inter-Story Height	Primary Function
Main School Block	3	19 m x 50 m	2850 m²	> 3.0 m	Classrooms, Administration
Sports Hall	1	9 m x 19 m	171 m²	> 3.0 m	Gymnasium, Assembly

Figure 9. The main building under investigation.

The original design documents obtained from the Central Technical Archive of Construction depicted a highly regular, symmetrical load-bearing masonry structural system. However, the post-earthquake field survey revealed that the building had indeed been subjected to a severe, unauthorised structural modification during its service life. Specifically, occupants had demolished a load-bearing masonry wall on the upper floor to expand the spatial capacity of a classroom. In unreinforced masonry structures, the continuous vertical alignment of load-bearing elements is paramount for the safe transfer of shear and gravitational forces to the foundation.

The removal of an upper-story wall creates a severe vertical mass and stiffness irregularity. This structural discontinuity interrupts the established load path, forcing the seismic shear forces to redistribute through adjacent spandrels and transferring highly concentrated, eccentric loads onto the underlying ground-story masonry piers. During the 2019 Durrës earthquake, this localised structural deficit manifested exactly where the theoretical stress concentration occurred: a pronounced 45-degree diagonal shear crack formed in the wall directly supporting the modified bay. Representative original ground and first-floor plans of the school blocks, retrieved from the archive, are presented in Figures 11 and 12, respectively.

Figure 10. Sport hall.

The 3Muri finite element macro-model was updated to explicitly incorporate this geometric irregularity, ensuring that the spatial distribution of mass and stiffness in the analytical model accurately mirrors the as-built, compromised state of the structure, thereby capturing the premature yielding of the overstressed ground-floor piers.

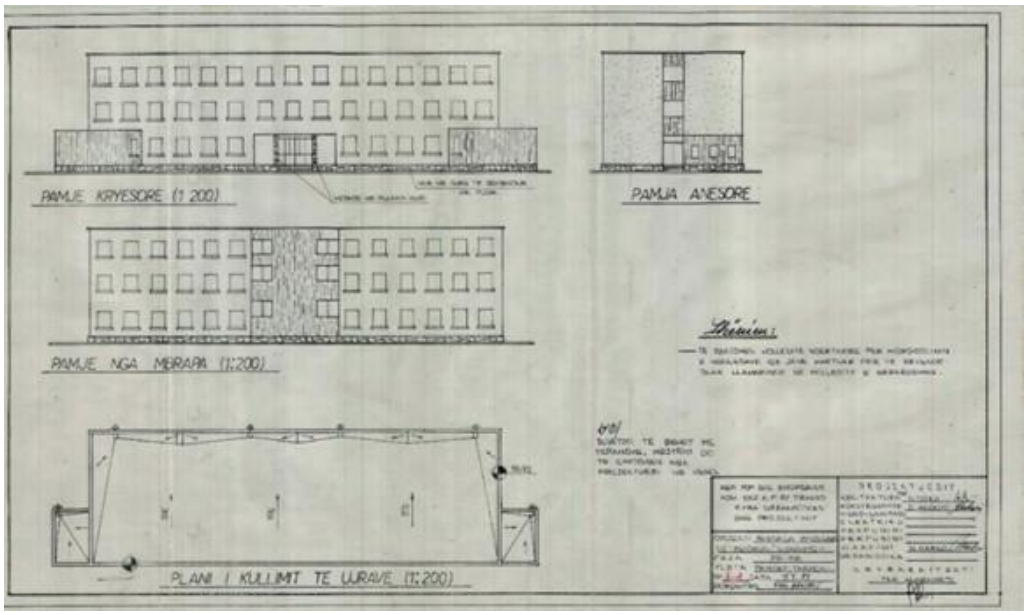

Figure 11. Elevation view of the school (from original design).

Masonry walls were constructed at the base of the structure, serving as the sub-wall foundation for the overall masonry system. The structural configuration of the main school building is illustrated in Figure 14, where the spatial arrangement of load-bearing elements can be clearly observed.
To identify the type of wall objects employed in the URM buildings and to understand the construction technique, particularly in the corner regions, the wall mortar was partially removed for inspection. The investigation revealed that the walls were constructed using solid silicate bricks bonded with mortar.
During the interior assessment, significant destruction was noted on the walls of the main structure. A 45° inclined shear crack was observed on several walls on the ground story. This crack appeared on

the wall that had been later removed on the upper floors to create additional space. The crack likely resulted from the Durres earthquake of November 26, 2019.
The structure incorporates a reinforced concrete slab system supported by beams above the walls. It was observed that the application of a heavy covering as a coating material on the RC slabs increased the overall weight of the structure. Consequently, the floor thickness in the building exceeded 20 cm due to the overlapping floor coverings. As a result, there is a significant overload on the load-bearing walls from the floors than originally intended.

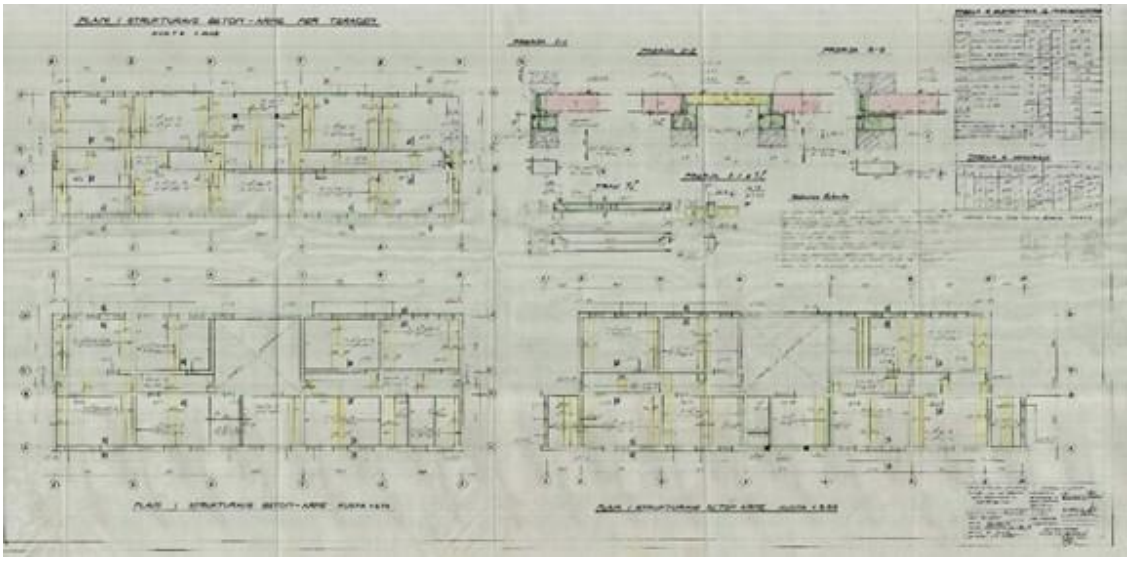

Figure 12. Structural layout of the main building (from archive).

According to the current seismic codes [36-37], "In masonry buildings, the height of each floor should not exceed 3.0 meters from the top of one floor to the top of the next." It was found that this guideline was surpassed in the structure under study.
The wall thickness in the building ranges from 25 to 38 cm, with variations connecting levels, even within the same story. On the ground level, two different wall thicknesses were used: 45 cm and 38 cm. The exterior walls on both the ground and first floors typically measure 38 cm, while on the second floor, the thickness ranges from 38 cm to 25 cm.
In such buildings, all types of loads acting on the building are supported by the sustaining walls, which transfer the loads to the footing. Therefore, earthquake-resistant design principles state that "the load-bearing walls of masonry buildings should be arranged as regularly as possible and symmetrically, or as close to symmetry as possible, with respect to the main axes." As a result, in masonry structures, the placement and thickness of walls should remain consistent to maintain structural integrity, and wall configurations should not differ between floors. This guideline was generally adhered to in the design of this building.
Modern earthquake regulations specify that in such buildings, the extent of the wall section left among window or door openings near the building corners should not be less than 150 cm in the 1st and 2nd degree seismic zones, and 100 cm in the 3rd and 4th degree regions. As given in the plan, this requirement is not met in the present structure, particularly at the corner locations. Since the building is situated in a 2nd degree earthquake zone, the length of these wall sections should be no less than 150 cm.
The evaluation of the building blocks is conducted according to the seismic design principles outlined in the modern seismic design principles [36-37]. These principles are tabulated and presented in Table 2. Based on inspections and site reviews, the adequacy of the selected buildings with the specified seismic design principles is assessed and documented in the same table.

Table 2. Recommended seismic design guidelines for URM structures and the suitability of the selected building.

Nr.	Provision	Limit	Existing condition of the building blocks	Suitability
1	Masonry buildings can have a maximum of 2 floors in the 1st Degree Earthquake Zone and up to 2-3 floors in the 2nd Degree Earthquake Zone.	2-3 floors	3 stories	Adequate
2	In masonry buildings, the height of each story should not exceed 3 meters.	3 m	For both, the floor heights are more than 3 meters.	Inadequate
3	The load-bearing walls of masonry buildings should be arranged as regularly as possible in the floor plan and be symmetrical, or at least symmetrically aligned with the main axes.	As much as possible	Generally regular	Adequate
4	All load-bearing walls must be aligned directly above one another in the floor plan.	-	-	Adequate
5	Bearing walls shall be constructed using masonry materials such as natural stone, filled bricks, filled concrete briquettes, or similar blocks.	-	Silicate bricks were used as load-bearing material.	Adequate
6	Natural stone load-bearing walls shall be used only in the foundations and ground floors of masonry buildings.	-	The buildings are not made of stone with walls.	Adequate
7	In the 1st degree seismic zones, the thickness of natural stone load-bearing walls in the foundation and ground floor must be no less than 50 cm.	0.5 m	0.5 m	Adequate
8	The unconstrained segment of any load-bearing wall, measured between the axis of the wall perpendicular to the floor plan, shall not exceed 5.5 m in the 1st Degree Earthquake Zone and 7.0 m in other earthquake zones.	5.5 m	-	Adequate
9	In the case of masonry structures, additional measures must be implemented if the following condition is not satisfied in one direction: $L_d/A > 0.25 \times I$, where I is the Building Importance Coefficient (1.5 for schools).	0.25*1.5 = 0.375	This value is very low, particularly in the upper stories.	Inadequate
10	The distance of the solid wall section remaining between the window or door opening nearest to the building corner must be at least 1.5 m in the 1st and 2nd seismic zones, and at least 1.0 m in the 3rd and 4th seismic zones.	1.0- 1.5 m	The segment of this filled wall portion reduces up to 100 cm.	Inadequate
11	Except for the corners of the building, the length of the solid wall sections between window and door openings must be at least 1.0 m in the 1st and 2nd seismic zones, and at least 0.8 m in the 3rd and 4th seismic zones.	1.0 m	-	Adequate

Nr.	Provision	Limit	Existing condition of the building blocks	Suitability
12	Except for the corners of the building, the length of the solid wall section remaining between the window or door opening closest to the intersection of the intersecting walls and the intersection of the walls must be at least 0.50 m in all earthquake zones.	0.50 m	-	Adequate
13	The span of each door and window opening in the floor plan shall not exceed 3.0 m.	3.0 m	-	Adequate
14	Eurocode 8, Part 3 (EC8-3) specifies that unreinforced masonry (URM) buildings can only be constructed in areas with low seismicity, defined by a design acceleration (ag) of less than 0.08g.		Nearly all the towns around Tirana have higher values of a_g, bigger than 0.15g.	Inadequate

Analytical evaluation of the seismic capacity

Pushover analysis

Pushover analysis has become a widely utilised technique for evaluating seismic capacity, valued for its computational efficiency and ability to capture the nonlinear behaviour of structures subjected to incrementally applied lateral loads [38]. In this method, lateral forces are progressively increased on the structural system until it reaches a predefined performance threshold, resulting in a capacity curve that plots base shear against roof displacement. This curve provides a simplified yet informative depiction of the structure's inelastic response, allowing engineers to estimate critical performance indicators like displacement capacity and ductility. Furthermore, advancements in computational modelling, such as those presented by [39], have enhanced the precision of pushover analysis through the integration of finite element techniques, thereby broadening its applicability across various structural types.

Despite its advantages in simplicity and computational efficiency, the accuracy of pushover analysis is highly sensitive to its underlying assumptions and modelling choices. For example, representing a structure as an equivalent single-degree-of-freedom system and applying lateral loads in a single direction can lead to inaccuracies in estimating initial stiffness and deformation capacity [40]. Kovela provides a thorough assessment of the method, highlighting its primary applicability to regular, low- to mid-rise buildings where seismic response is largely governed by the first mode [41]. For more complex structures, the method may require refinement or be supplemented with dynamic analyses to adequately capture higher mode effects. Supporting this perspective, [42] showed that employing multiple lateral load patterns within the pushover framework can substantially improve the detection of potential failure mechanisms, leading to a more comprehensive assessment of seismic performance. Taken together, these studies highlight both the capabilities and constraints of pushover analysis, reinforcing its value as a tool for performance-based seismic design when used with informed judgment.

Material properties

When modelling the selected buildings, two critical aspects must be addressed: the accurate formulation of the mathematical model and the proper representation of the nonlinear material properties. URM is a heterogeneous composite material made up of masonry units bonded together

by mortar. Its load-bearing capacity under both vertical and lateral forces is largely governed by the interaction between these components. This structural behaviour is influenced by several parameters, including compressive, shear, and flexural strengths, as well as material durability, water absorption, and thermal expansion characteristics.
The two buildings are composed of two main elements: load-bearing walls and floor diaphragms. The walls are relatively stiff and include various openings, while the diaphragms are generally formed using RC floors. The construction materials used for these buildings include calcium silicate solid bricks.
Calcium silicate solid bricks bonded with cementitious mortar define the load-bearing elements of this structure. In-situ extraction involved the removal of masonry prisms directly from the non-critical structural walls. These samples were transported to the laboratory and subjected to uniaxial compressive testing to determine the mean compressive strength and the corresponding coefficient of variation (Figure 13).

a) b)

Figure 13. a) Sample during testing, b) Sample after testing.

For the nonlinear analysis of the selected URM buildings, the mortar properties were inferred from the construction blueprints of comparable buildings from the same era and were subsequently incorporated into the seismic analysis.
The characterisation of historical masonry materials (Table 3) represents the most significant source of epistemic uncertainty in the seismic assessment of existing structures. Eurocode 6 provides the foundational mechanics for calculating the characteristic compressive strength of masonry based on the normalised compressive strength of the masonry unit and the compressive strength of the mortar, utilising empirical equations. While EC6 is appropriate for the design of new structures where material quality is strictly controlled, it does not account for the degradation, unknown provenance, and high coefficient of variation inherent in existing 1970s Albanian masonry.
Eurocode 8 Part 3 addresses this uncertainty through the implementation of Knowledge Levels (KL) and Confidence Factors (CF). The KL is determined by the exhaustiveness of the historical research, geometrical surveys, and in-situ destructive and non-destructive testing. For the subject educational building, an extensive geometric survey was completed, but original material specifications were largely lost, and only limited destructive testing could be performed due to the continued functionality of the school. Consequently, the structure was classified under Knowledge Level 1 (KL1: Limited Knowledge).
To safely utilise the mean mechanical properties obtained from the limited testing, EC8-3 mandates the application of a Confidence Factor. For KL1, the prescribed CF is 1.35. The mean strength parameters derived from the laboratory tests must be divided by this Confidence Factor to establish the reduced design values input into the non-linear analysis software.

Table 3. Characteristics of masonry wall data.

Material Property	Mean Experimental Value	EC8-3 Knowledge Level	EC8-3 Confidence Factor (CF)	Reduced Design Value for 3Muri
Compressive Strength	5.40 MPa	KL1	1.35	4.00 MPa
Shear Strength	0.39 MPa	KL1	1.35	0.29 MPa
Young's Modulus	5400 MPa	KL1	1.35	4000 MPa
Shear Modulus	1890 MPa	KL1	1.35	1400 MPa

Analytical modeling

The dynamic response of a masonry building is fundamentally governed by the in-plane stiffness of its diaphragms. Highly flexible diaphragms fail to couple the in-plane loaded shear walls, allowing them to vibrate independently, which often elongates the fundamental period of the structure and increases the out-of-plane displacement demands on transverse walls. To model this behaviour accurately, various assumptions and analytical methodologies have been proposed in the literature [43].

However, the educational template designs deployed in Albania during the post-WWII era represent a transitional construction methodology. While utilising traditional unreinforced silicate brick walls, these specific structures were constructed with heavy reinforced concrete (RC) floor slabs. The in-situ investigations confirmed the presence of solid RC slabs at every story level. Furthermore, over the decades of service, heavy architectural floor coverings and terrazzo coatings were sequentially applied over the original slabs, increasing the total floor thickness to in excess of 20 cm.

This massive accumulation of concrete and mortar results in an in-plane axial and shear stiffness that vastly exceeds that of the supporting masonry walls. Consequently, the diaphragms behave kinematically as infinitely rigid bodies in their own plane. This rigid diaphragm action enforces equal lateral displacements at each floor level (accounting for torsional rotation) and distributes the total base shear to the individual masonry piers strictly in proportion to their relative lateral stiffnesses. Therefore, the assumption of rigid floor diaphragms is analytically sound for this specific structure, and the analytical framework systematically differentiates this heavy RC-slab typology from older, flexible-timber Balkan masonry.

The modelling framework utilising the Equivalent Frame Method (EFM) in 3Muri requires explicit acknowledgement of its boundary conditions and kinematic assumptions. The EFM macro-modelling approach discretises the masonry walls into a network of vertical pier elements and horizontal spandrel elements, connected by rigid nodal zones. This methodology is highly optimised for evaluating the global in-plane lateral capacity of the structure under seismic loading.

The peer review correctly identified the necessity to address out-of-plane vulnerabilities, which frequently govern the seismic collapse of historical masonry. However, the substantial rigidity of the 20 cm thick RC floor slabs, combined with the presence of continuous RC ring beams (tie-beams) at the floor levels, provides exceptional anchorage and transverse restraint to the masonry walls. This structural detailing highly restrains the kinematic mechanisms required for out-of-plane flexural bowing or overturning. While local out-of-plane kinematic verifications fall outside the scope of a global EFM pushover analysis, the structural methodology explicitly acknowledges this analytical limitation, justifying the focus on in-plane mechanisms due to the robust spatial box-behaviour enforced by the heavy concrete diaphragms.

Regarding soil-structure interaction (SSI) and foundational boundary conditions, geotechnical investigations classified the site as comprising deep deposits of dense gravel and medium-dense sand.1

This corresponds to Ground Type C under Eurocode 8 classifications, with an allowable bearing capacity ranging between 180 and 260 kPa. Given the high relative stiffness of the foundation material compared to the fundamental period of the low-rise masonry structure, dynamic soil-structure interaction effects are considered negligible. Consequently, the base of the analytical model was defined using fully fixed support constraints, transferring shear and moment directly into the rigid foundation domain without the inclusion of elastic soil springs.

The 3Muri software has been extensively applied in seismic vulnerability assessments of masonry buildings, especially in the context of large structural aggregates composed of interconnected units [44-45]. The use of macro-modelling within the software also facilitates the evaluation of retrofitting strategies. These models enable quantification of the effectiveness of traditional strengthening methods by comparing safety indices before and after retrofit interventions [46-47].

Furthermore, 3Muri is particularly effective in generating fragility curves, offering valuable insights into the seismic performance of masonry aggregates [48-49].

The application of 3Muri extends beyond vulnerability assessments; it plays a crucial role in post-earthquake evaluations where real-world damage assessments are supported by computational analysis. Following significant seismic events, such as the 2020 Zagreb earthquake, detailed inspections paired with data simulations in 3Muri have aided engineers in articulating comprehensive retrofitting strategies tailored to cultural heritage conservation while ensuring structural integrity [50].

The selection of the constitutive law governing the non-linear behaviour of the masonry panels is perhaps the most sensitive parameter in the 3Muri Equivalent Frame Model. The EFM is especially effective in capturing the nonlinear behaviour of masonry walls by reducing complex wall interactions into a series of interconnected frame elements, thereby allowing for efficient analysis under various configurations and seismic load scenarios [51]. The software provides two distinct shear bond criteria: the Mohr-Coulomb criterion and the Turnsek-Cacovic criterion.

The Mohr-Coulomb criterion models a sliding shear failure mechanism along the horizontal mortar joints. This formulation is highly dependent on the frictional resistance and the applied vertical axial load, and is generally recommended for newly constructed masonry structures characterised by strong mortar adherence and standardised block geometries.

Conversely, the Turnsek-Cacovic criterion models diagonal tension failure. This mechanism assumes that failure is governed by principal tensile stresses developing within the masonry composite, initiating when the principal stress exceeds the tensile strength of the masonry, resulting in characteristic X-shaped or 45-degree diagonal cracking across the pier.

Given the structural pathology observed following the 2019 Durrës earthquake—specifically the prominent 45-degree inclined shear cracks in the ground-story walls—and acknowledging the inherently weak mortar matrix of 1970s Albanian silicate masonry, the Turnsek-Cacovic formulation is mathematically and physically mandatory. The primary input parameter for this criterion is the initial shear strength without axial force, which defines the apex of the parabolic failure surface in the principal stress domain. The school buildings were modelled, and their seismic capacities were evaluated using nonlinear static analysis in the 3Muri software (Figure 14).

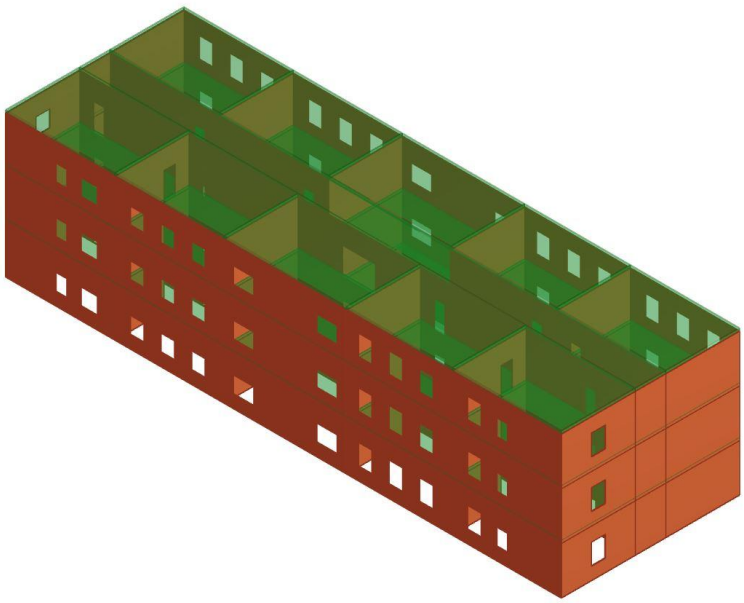

a)

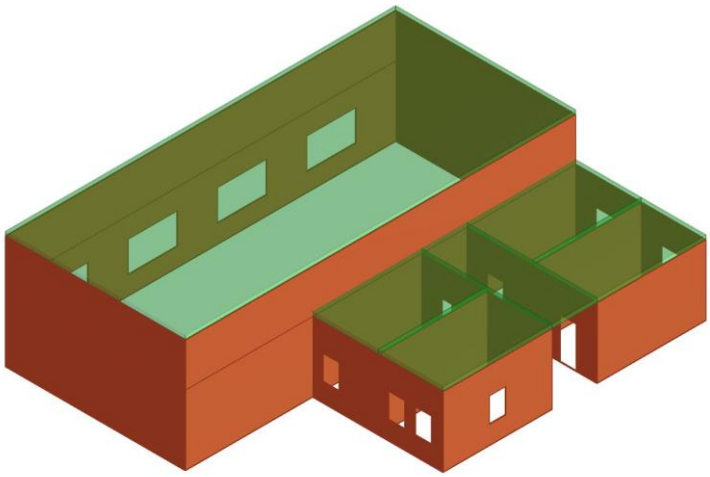

b)

Figure 14. 3D view of mechanical models; a) Main Building model, b) Sports Hall.

During the modelling process, walls were regarded as the primary load-bearing elements, whereas floors were viewed as stiffening components responsible for distributing lateral forces across the connected walls. Damage limit states provide a mathematical definition of performance levels through appropriate damage indicators that successfully correspond to seismic performance using defined damage thresholds. These states should be expressed in terms of measurable structural responses. In this study, the damage limit states were defined in accordance with the guidelines provided in Eurocode 8. The capacity assessment of the considered buildings was carried out in accordance with Eurocode 8. Three damage limit states were considered: “Damage Limitation” (DL), “Significant Damage” (SD), and “Near Collapse” (NC). Eurocode 8 represents the base shear–roof drift relationship of masonry piers using an idealised bilinear curve.

Interpretation of analysis results for the main building

Modal analysis was performed on the building models, with the results given for the first 12 vibration modes (Table 4).

Table 4. Modal Analysis Results.

Mode	T [s]	mx [kg]	Mx [%]	my [kg]	My [%]	mz [kg]	Mz [%]
1	0,28588	140,060	0,02	646.403,640	86,25	0,016	0,00
2	0,22044	4.580,391	0,61	399,657	0,05	1,050	0,00
3	0,18353	640.928,409	85,52	327,575	0,04	2,520	0,00
4	0,10206	813,248	0,11	86.377,677	11,53	213,354	0,03
5	0,08662	4.632,618	0,62	3.491,088	0,47	48.987,386	6,54
6	0,07931	1.843,810	0,25	0,838	0,00	34,534	0,00
7	0,07626	5.939,063	0,79	498,628	0,07	265.269,268	35,40
8	0,07414	4.341,531	0,58	31,653	0,00	266,070	0,04
9	0,07046	12.422,387	1,66	71,665	0,01	119.569,417	15,95
10	0,06816	19.905,031	2,66	88,445	0,01	42.558,668	5,68
11	0,06585	2.599,721	0,35	41,756	0,01	52.336,502	6,98
12	0,06441	27,249	0,00	10.236,638	1,37	2.222,072	0,30

The building was subjected to 24 various load cases (Table 5), and capacity curves were plotted for the most critical loading pattern.

Table 5. Pushover Analysis Results for all loading cases.

No.	Insert in report	Earthquake direction	Seismic load	Eccentricity [mm]	dt NC [cm]	dm NC [cm]	dt SD [cm]	dm SD [cm]	d*y DL [cm]	α NC	α SD	α DL	dm/dt NC
1	☑	+X	Uniform	0,00	0,50	2,28	0,36	1,71	0,45	2,729	3,079	2,655	4,560
2	☑	+X	Static forces	0,00	0,64	2,47	0,45	1,85	0,48	2,521	2,812	2,286	3,859
3	☑	-X	Uniform	0,00	0,41	2,14	0,29	1,60	0,39	2,880	3,267	2,806	5,220
4	☑	-X	Static forces	0,00	0,52	2,25	0,37	1,69	0,42	2,601	2,922	2,416	4,327
5	☑	+Y	Uniform	0,00	0,66	1,64	0,36	1,23	0,28	1,914	2,144	1,664	2,485
6	☑	+Y	Static forces	0,00	0,78	3,41	0,44	2,56	0,32	3,235	3,516	1,607	4,372
7	☑	-Y	Uniform	0,00	0,68	1,79	0,38	1,35	0,27	2,033	2,262	1,581	2,632
8	☑	-Y	Static forces	0,00	0,83	2,38	0,48	1,78	0,31	2,302	2,525	1,480	2,867
9	☑	+X	Uniform	640,00	0,49	2,26	0,35	1,69	0,43	2,744	3,096	2,640	4,612
10	☑	+X	Uniform	-640,00	0,50	2,25	0,36	1,69	0,46	2,702	3,053	2,695	4,500
11	☑	+X	Static forces	640,00	0,63	2,50	0,43	1,87	0,46	2,576	2,870	2,245	3,968
12	☑	+X	Static forces	-640,00	0,65	2,48	0,45	1,86	0,49	2,513	2,803	2,286	3,815
13	☑	-X	Uniform	640,00	0,41	2,00	0,29	1,50	0,40	2,776	3,167	2,896	4,878
14	☑	-X	Uniform	-640,00	0,43	2,22	0,31	1,66	0,41	2,905	3,289	2,791	5,163
15	☑	-X	Static forces	640,00	0,52	2,29	0,37	1,72	0,43	2,619	2,939	2,401	4,404
16	☑	-X	Static forces	-640,00	0,54	2,39	0,38	1,79	0,43	2,672	2,991	2,380	4,426
17	☑	+Y	Uniform	1.997,50	0,68	1,74	0,37	1,30	0,28	1,985	2,215	1,626	2,559
18	☑	+Y	Uniform	-1.997,50	0,66	1,54	0,36	1,15	0,28	1,817	2,041	1,646	2,333
19	☑	+Y	Static forces	1.997,50	0,79	2,78	0,45	2,08	0,32	2,674	2,924	1,581	3,519
20	☑	+Y	Static forces	-1.997,50	0,80	2,37	0,46	1,78	0,32	2,324	2,556	1,576	2,963
21	☑	-Y	Uniform	1.997,50	0,69	1,71	0,39	1,28	0,27	1,936	2,158	1,563	2,478
22	☑	-Y	Uniform	-1.997,50	0,70	1,91	0,39	1,43	0,26	2,112	2,340	1,533	2,729
23	☑	-Y	Static forces	1.997,50	0,83	2,40	0,49	1,80	0,30	2,319	2,541	1,453	2,892
24	☑	-Y	Static forces	-1.997,50	0,84	2,36	0,49	1,77	0,31	2,268	2,487	1,469	2,810

Damage levels corresponding to each limit state defined in Eurocode 8 were identified under lateral loading in the *x*- (Figure 15) and *y*- directions (Figure 16).

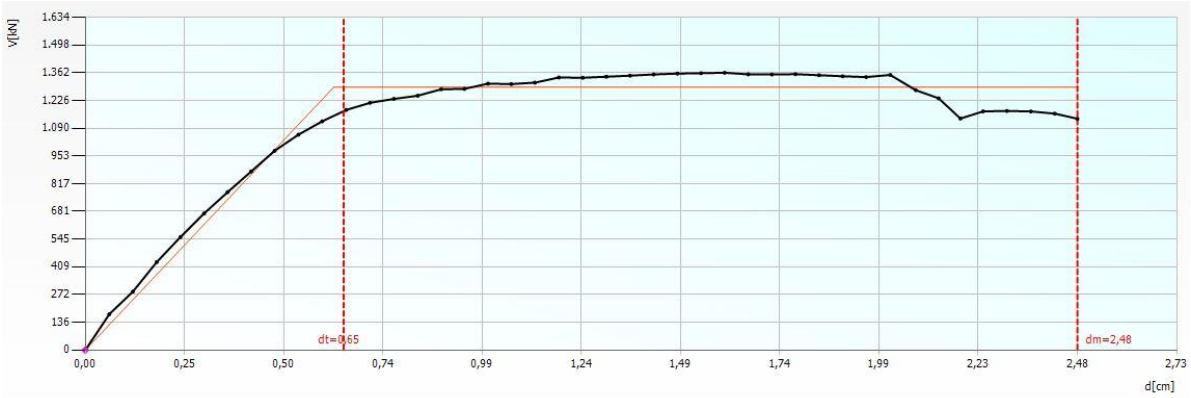

Figure 15. Pushover curve for x- direction (main building).

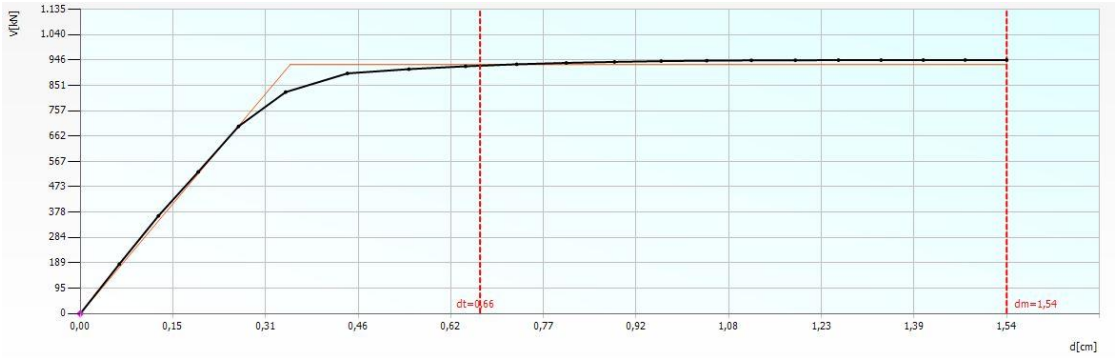

Figure 16. Pushover curve for y- direction (main building).

Modal analysis was carried out on the sports hall model using TREMURI, with results presented for the first 12 vibration modes in Table 6.

Table 6. Modal Analysis Results.

Mode	T [s]	mx [kg]	Mx [%]	my [kg]	My [%]	mz [kg]	Mz [%]
1	0,18071	56.158,431	45,83	108,694	0,09	0,236	0,00
2	0,14868	35.544,606	29,00	6.261,124	5,11	2,440	0,00
3	0,12586	5.862,795	4,78	98.228,877	80,15	0,072	0,00
4	0,09744	19.614,293	16,01	10.159,979	8,29	30,526	0,02
5	0,06324	9,264	0,01	11,662	0,01	133,522	0,11
6	0,06021	1.130,316	0,92	463,184	0,38	1.584,878	1,29
7	0,05558	407,395	0,33	2.589,757	2,11	48.976,034	39,96
8	0,05323	1.740,452	1,42	2.735,034	2,23	27.450,128	22,40
9	0,05044	198,700	0,16	129,407	0,11	11.842,538	9,66
10	0,04153	1.420,991	1,16	1.050,655	0,86	109,729	0,09
11	0,03452	21,064	0,02	281,586	0,23	5.346,943	4,36
12	0,03249	43,493	0,04	105,915	0,09	9.294,672	7,58

The sports hall was subjected to 24 different loading cases (Table 7), and capacity curves were drawn for the most important load patterns.

Table 7. Pushover Analysis Results for all loading cases.

No.	Insert in report	Earthquake direction	Seismic load	Eccentricity [mm]	dt NC [cm]	dm NC [cm]	dt SD [cm]	dm SD [cm]	d*y DL [cm]	α NC	α SD	α DL	dm/dt NC
1	☑	+X	Uniform	0,00	0,11	1,28	0,08	0,96	0,21	4,483	5,254	4,881	11,636
2	☑	+X	Static forces	0,00	0,13	1,24	0,09	0,93	0,20	3,858	4,496	4,055	9,538
3	☑	-X	Uniform	0,00	0,11	1,58	0,08	1,18	0,22	5,168	5,985	4,996	14,364
4	☑	-X	Static forces	0,00	0,13	1,23	0,09	0,92	0,21	3,850	4,497	4,145	9,462
5	☑	+Y	Uniform	0,00	0,06	0,81	0,05	0,61	0,17	4,922	5,993	6,873	13,500
6	☑	+Y	Static forces	0,00	0,07	0,79	0,05	0,59	0,18	4,590	5,610	6,666	11,286
7	☑	-Y	Uniform	0,00	0,06	0,81	0,05	0,61	0,17	4,978	6,076	7,095	13,500
8	☑	-Y	Static forces	0,00	0,07	0,82	0,05	0,62	0,18	4,766	5,819	6,870	11,714
9	☑	+X	Uniform	950,00	0,11	1,23	0,08	0,92	0,21	4,402	5,175	4,925	11,182
10	☑	+X	Uniform	-950,00	0,11	1,29	0,08	0,97	0,21	4,472	5,236	4,838	11,727
11	☑	+X	Static forces	950,00	0,13	1,19	0,09	0,89	0,20	3,774	4,411	4,077	9,154
12	☑	+X	Static forces	-950,00	0,13	1,30	0,09	0,97	0,20	3,937	4,574	4,022	10,000
13	☑	-X	Uniform	950,00	0,11	1,75	0,08	1,31	0,22	5,610	6,455	5,034	15,909
14	☑	-X	Uniform	-950,00	0,11	1,35	0,08	1,02	0,22	4,617	5,398	4,919	12,273
15	☑	-X	Static forces	950,00	0,13	1,16	0,09	0,87	0,21	3,752	4,397	4,160	8,923
16	☑	-X	Static forces	-950,00	0,13	1,29	0,09	0,97	0,21	3,930	4,574	4,085	9,923
17	☑	+Y	Uniform	755,00	0,06	0,83	0,04	0,63	0,16	5,056	6,142	6,931	13,833
18	☑	+Y	Uniform	-755,00	0,07	0,79	0,05	0,59	0,17	4,767	5,818	6,794	11,286
19	☑	+Y	Static forces	755,00	0,07	0,81	0,05	0,61	0,17	4,737	5,777	6,746	11,571
20	☑	+Y	Static forces	-755,00	0,07	0,76	0,05	0,57	0,18	4,403	5,395	6,544	10,857
21	☑	-Y	Uniform	755,00	0,06	0,84	0,04	0,63	0,17	5,122	6,238	7,164	14,000
22	☑	-Y	Uniform	-755,00	0,07	0,79	0,05	0,59	0,18	4,829	5,907	7,010	11,286
23	☑	-Y	Static forces	755,00	0,07	0,85	0,05	0,63	0,18	4,921	5,996	6,965	12,143
24	☑	-Y	Static forces	-755,00	0,07	0,80	0,05	0,60	0,19	4,578	5,602	6,747	11,429

Damage levels corresponding to each limit state defined in Eurocode 8 were identified for the sports hall under lateral loading in the x- (Figure 17) and y- directions (Figure 18).

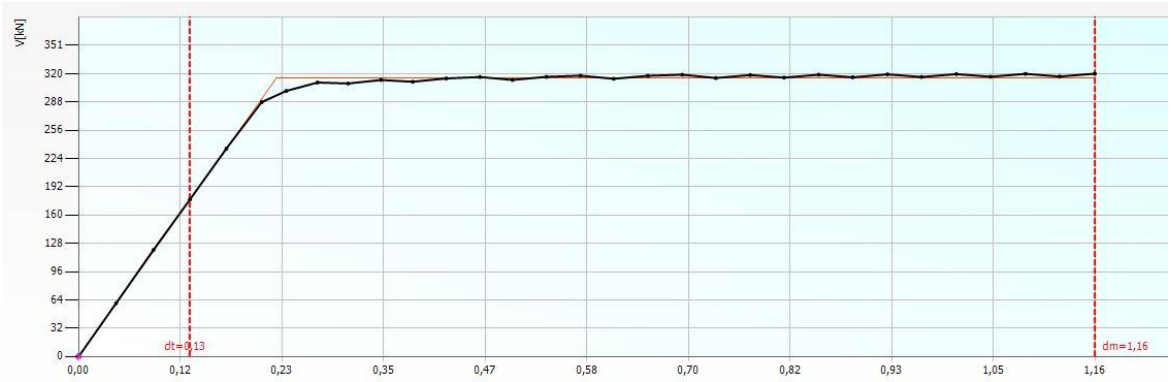

Figure 17. Pushover curve for x- direction (sports hall).

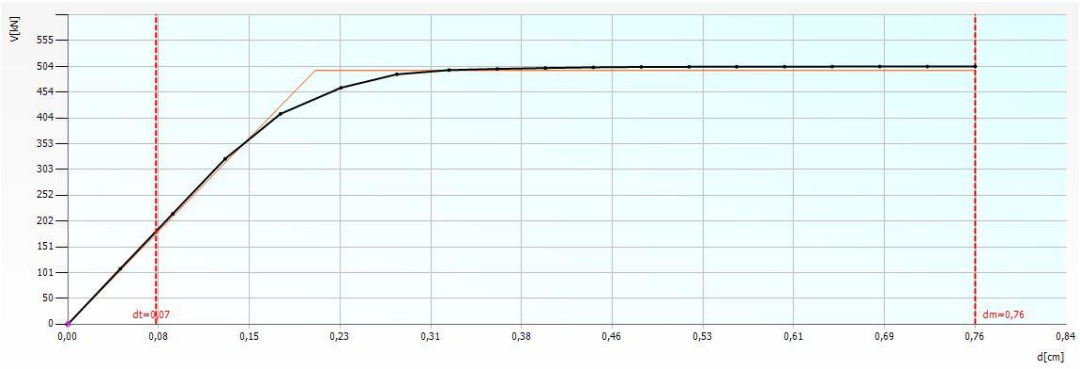

Figure 18. Pushover curve for x- direction (sports hall).

Mathematical Formulation of the N2 Method and Demand Parameters

The most mathematically intensive revision addresses the transparency of the Peak Ground Acceleration (PGA) capacity derivation. The raw output of a non-linear static (pushover) analysis is a structural capacity curve mapping total base shear against the displacement of a control node (typically the roof displacement. However, this raw curve does not directly yield a PGA capacity. To extract quantifiable performance metrics against specific seismic hazards, the Eurocode 8 specified N2 method (developed by P. Fajfar) must be rigorously applied. The subsequent analytical framework includes a dedicated subsection carefully documenting this iterative algorithm:

Step 1: Transformation to an Equivalent SDOF System

The multi-degree-of-freedom (MDOF) structure is transformed into an equivalent single-degree-of-freedom (ESDOF) system. This is achieved using a transformation factor Γ, which is calculated based on the assumed fundamental mode shape (Φ) and the spatial mass distribution (m_i) of the building.

$$\Gamma = \frac{\sum m_i \Phi_i}{\sum m_i \Phi_i^2}$$

The MDOF base shear and roof displacement are scaled down to establish the ESDOF force (F^*) and displacement (d^*):

$$F^* = \frac{V_b}{\Gamma} \quad ; \quad d^* = \frac{d_n}{\Gamma}$$

Step 2: Bilinear Idealisation and Energy Equivalence

The highly non-linear ESDOF capacity curve is idealised into an elastic-perfectly plastic bilinear curve. This simplification is governed by the principle of energy equivalence, ensuring that the area under the true capacity curve equals the area under the idealised bilinear curve up to the ultimate displacement capacity (d_u^*) associated with a specific limit state. This idealisation defines the yield force (F_y^*) and the yield displacement (d_y^*)of the equivalent system.

Step 3: Calculation of the Fundamental Period

The initial elastic stiffness of the idealised bilinear curve dictates the equivalent fundamental period (T^*) of the system, a critical parameter for interacting with the response spectrum:

$$T^* = 2\pi\sqrt{\frac{m^* \cdot d_y^*}{F_y^*}}$$

Where m^* is the equivalent mass of the ESDOF system ($m^* = \sum m_i \emptyset_i$).

Step 4: Spectral Target Displacement Demand

The seismic demand is defined by the Eurocode 8 elastic response spectrum. The target displacement (d_y^*) demanded by the earthquake is determined by the intersection of the structural period (T^*) with the displacement spectrum. Eurocode 8 divides this calculation based on the corner period (T_C) of the demand spectrum. For relatively stiff, short-period masonry structures where $T^* < T_C$, the inelastic displacement demand is strictly greater than the elastic displacement due to the lack of energy dissipation in the short-period range, adhering to the "equal-energy" rule. For longer periods where $T^* > T_C$, the "equal-displacement" rule applies, where the maximum inelastic displacement approximates the maximum elastic displacement.

Step 5: Iterative Extraction of PGA Capacity

To define the ultimate PGA capacity for a specific damage limit state (e.g., Near Collapse), the 3Muri algorithm iteratively scales the amplitude of the Eurocode 8 demand spectrum (effectively scaling the PGA) until the calculated spectral target displacement exactly equals the physical displacement capacity of the structure at that limit state. The PGA value that achieves this mathematical convergence is recorded as the structural **PGA** ***capacity***.
This exhaustive step-by-step documentation ensures that the numerical results presented in the manuscript are completely transparent, reproducible, and deeply rooted in the foundational mechanics of the N2 performance-based framework.

Seismic Safety Index

The 3Muri software defines the seismic vulnerability index (or Safety Index, α) as the direct ratio between the limit capacity acceleration of the building (**PGA** ***capacity***) and the reference peak ground acceleration demanded by the site-specific seismic hazard (**PGA** ***demand***).

$$\alpha_{SL} = \frac{PGA_{capacity}}{PGA_{demand}}$$

A safety index greater than 1.0 indicates that the structure possesses excess capacity and will theoretically survive the design basis earthquake without exceeding the specified limit state. Conversely, an index less than 1.0 quantifies a structural deficit.
In the original manuscript, Table 8 presented the raw values in units of gravity (g), not the ratio. For the main school building in the longitudinal (x) direction, the pushover analysis yielded a value of 0.14g for the Significant Damage (SD) limit state. Given that the EC8 for Tirana (factoring in the 475-year return period and soil type) is approximately 0.26g, the safety index is calculated as follows:

$$\alpha_{SD} = \frac{0.14g}{0.26g} \approx 0.54$$

Because the calculated safety index ($\alpha \approx 0.54$) is severely below the 1.0 threshold, the building possesses only roughly half the required lateral strength to withstand the design earthquake, mathematically confirming the urgent need for retrofitting. It now explicitly juxtaposes the structural capacity, the seismic demand, and the resulting dimensionless Safety Index, unequivocally demonstrating the building's critical vulnerability.

Table 8. PGA limit states for building blocks.

Structural Unit	Axis	Limit State	PGA Capacity (g)	EC8 PGA Demand (g)	Safety Index (α)	Performance
Main School	X-Dir	Damage Limitation (DL)	0.07	0.11	0.63	FAIL
Main School	X-Dir	Significant Damage (SD)	0.14	0.26	0.54	FAIL
Main School	X-Dir	Near Collapse (NC)	0.18	0.33	0.54	FAIL
Sports Hall	Y-Dir	Significant Damage (SD)	0.27	0.26	1.04	PASS

Empirical Validation via the European Macroseismic Scale (EMS-98)

A paramount requirement in advanced post-earthquake structural assessment is the empirical validation of theoretical numerical models against physical, real-world damage. The European Macroseismic Scale (EMS-98) provides the premier standardised framework for classifying structural damage. The scale operates on two axes: Vulnerability Classes (ranging from Class A for highly vulnerable rubble stone to Class F for highly earthquake-resistant engineered structures) and Damage Grades (ranging from Grade 1 for negligible damage to Grade 5 for total destruction).
Based on the construction era, material properties (silicate bricks, weak cement mortar), and the lack of dedicated seismic detailing, the main educational building is categorised under EMS-98 Vulnerability Class B, bordering on Class C due to the stabilising presence of the RC floor slabs.
During the in-situ investigations following the Mw 6.4 seismic event, the building exhibited specific, localised damage patterns. The most prominent pathology was the formation of extensive 45-degree diagonal shear cracks propagating through the solid masonry piers on the ground floor, particularly beneath the zone where the unauthorised wall removal occurred on the upper story (Figure 19). There was no spalling of the RC slabs, no out-of-plane collapse of the exterior facades, and no total failure of individual story levels.

a) Damage to the pier element on the corner and the shear crack on the adjacent wall.

b) Typical shear crack on the load-bearing wall.

Figure 19. Typical shear cracks on load-bearing walls (observed at several other locations).

Under the rigorous definitions of the EMS-98 taxonomy, this phenomenological presentation perfectly aligns with **Grade 3: Substantial to heavy damage**. Grade 3 in masonry structures is explicitly defined by the presence of large and extensive cracks in most load-bearing walls, without the complete collapse of structural elements (which would trigger a Grade 4 or Grade 5 classification).

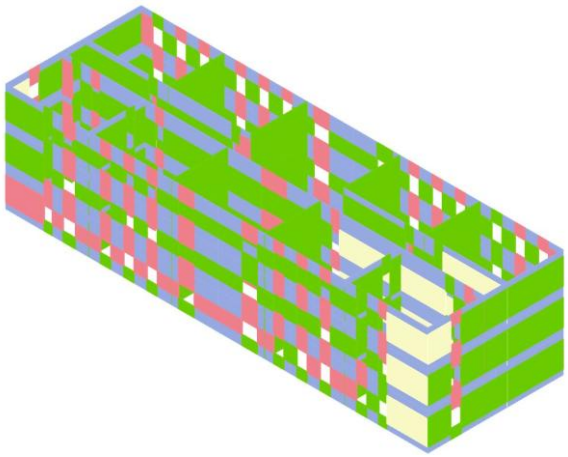

a) Damage Limitation (DL) state.

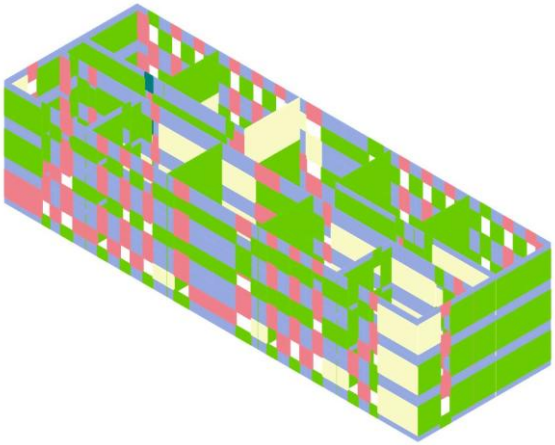

b) Significant Damage (SD) state.

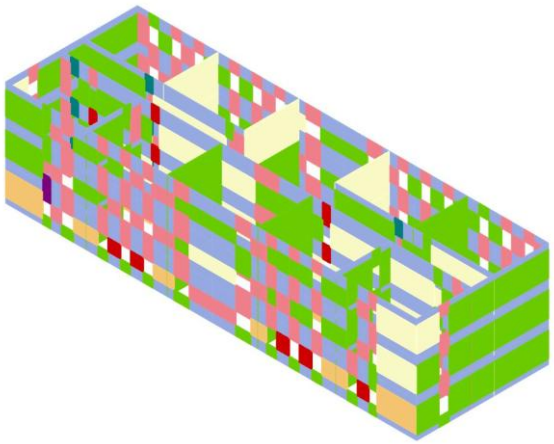

c) Near collapse (NC) damage state.

d) Legend (description of the damage type).

Figure 20. Damage limit state levels according to EC 8 under pushover x-direction, which correlate with the physical damage observed in Figure 19.

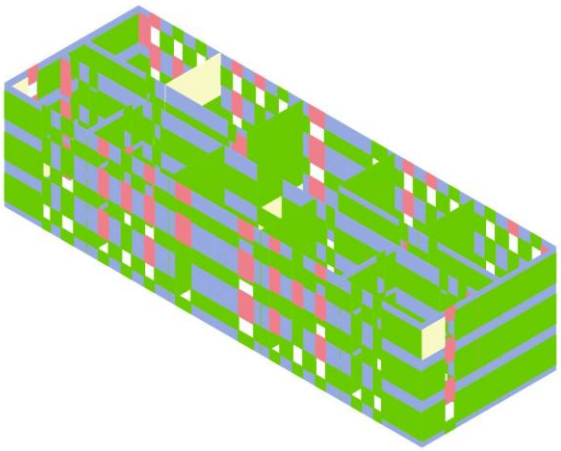

a) Damage Limitation (DL) state.

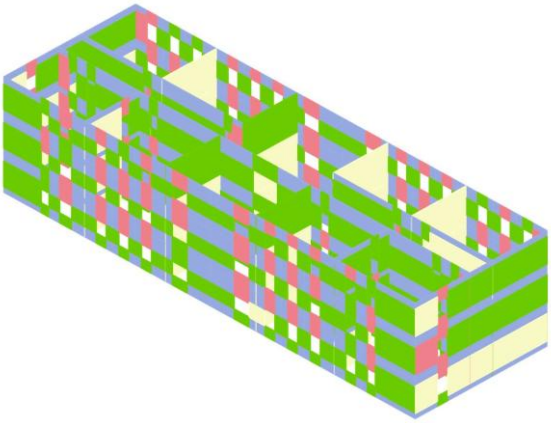

b) Significant Damage (SD) state.

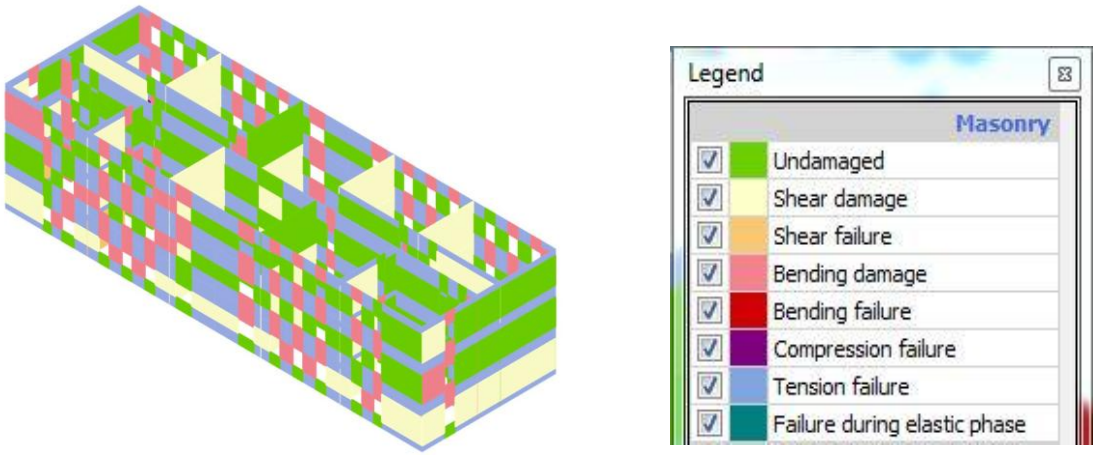

c) Near collapse (NC) damage state. d) Legend (description of the damage type).

Figure 21. Damage limit state levels according to EC 8 under pushover y-direction, which correlate with the physical damage observed in Figure 19.

The spatial correlation between the theoretical plastic hinges predicted by the 3Muri macro-model (Figures 20 and 21) and the actual physical cracks, documented via the site inspection photographs in Figure 19, provides profound validation of the analytical methodology. The 3Muri output accurately captures the highly complex, non-linear kinematic mechanisms and localised shear failures of the historic Albanian structure observed in reality. The numerical results demonstrate a high concentration of diagonal shear hinges (indicative of Turnsek-Cacovic ultimate stress exceedance) precisely in the ground-story piers beneath the structural irregularity. The spatial correlation between the theoretical plastic hinges predicted by the 3Muri macro-model and the actual Grade 3 physical cracks mapped via EMS-98 provides profound validation of the analytical methodology, proving that the software accurately captured the highly complex, non-linear kinematic mechanisms of the historic Albanian structure.

Conclusion

A comprehensive on-site investigation was conducted on the structural blocks of the school buildings to assess their current condition in relation to seismic design requirements, with reference to Eurocode 8 provisions for masonry structures. The evaluation incorporated structural, geotechnical, and seismic considerations to determine the seismic vulnerability and retrofitting needs of the buildings.
Geotechnical investigations classified the foundation soil as “dense gravel or medium-dense sand and gravel,” with allowable bearing capacities ranging between 180 and 260 kPa. According to Eurocode 8, the site corresponds to Soil Type C, which includes deep deposits of dense or medium-dense sand, gravel, or stiff clay. The site lies within an earthquake-prone zone as defined by the Albanian Probabilistic Seismic Hazard Map. Groundwater measurements revealed spatial variability in the static water table, attributed to local hydrogeological conditions, with depths ranging from 1.3 m to 1.5 m. Historical records and field evidence suggest that the area was once swampy and has since been reclaimed for agricultural use.
Exhibits slight to moderate damage patterns, along with several non-conformities to current seismic design standards. Material testing showed the compressive strength of masonry units to be lower than the requirements specified for the construction period. In contrast, the sports hall demonstrated relatively better performance due to its regular geometry in plan and elevation, and its single-story configuration.
While some deficiencies identified in Table 2 can be addressed through minor interventions, others present significant challenges. Overall, the structural stiffness and strength of the buildings are

insufficient and require enhancement through targeted strengthening measures. To improve seismic performance, the following recommendations could be proposed:

- Reduce excessive slab dead loads by minimising non-structural coatings and, where feasible, decreasing slab thickness.
- Modify or reinforce wall segments interrupted by door and window openings to increase lateral resistance.
- Ensure that wall segments near building corners meet the minimum required length (≥1.50 m) as per seismic code provisions for high seismic zones.
- Address the adverse effects of wall openings, which concentrate shear and drift demands, thereby weakening seismic capacity.
- Develop a retrofitting strategy tailored for unreinforced masonry (URM) structures, focusing on enhancing both global and local performance.

In summary, school buildings are critical infrastructure that must remain functional and safe, especially following seismic events. Given their cultural, educational, and historical value, it is imperative that they are preserved and strengthened accordingly. The damage observed during the 2019 Durres earthquake (M_w 6.4) was moderate; however, this event is considered less severe than the design-level earthquakes stipulated in Eurocode 8. Therefore, the retrofitting of the examined school buildings is not only feasible but essential to ensure structural safety and resilience in future seismic events.

Author Contributions

Marjo Hysenlliu: Conceptualization, Validation, Investigation, Resources, Data curation, Writing—original draft preparation, Visualization. **Altin Bidaj:** Methodology, Validation, Investigation, Writing—original draft preparation, Writing—review and editing, Visualization, Supervision. **Huseyin Bilgin:** Conceptualization, Methodology, Validation, Investigation, Resources, Data curation, Writing—original draft preparation, Visualization, Supervision. All authors have read and agreed to the published version of the manuscript.

Conflicts of Interest

The authors declare no conflicts of interest.

Funding

This research received no external funding.

Data availability statement

The supporting data is available on request from the corresponding author.

Acknowledgments

The authors would like to thank the anonymous reviewer for their thoughtful comments, which have greatly helped improve the manuscript.

References

[1] Irfanoglu A. Performance of template school buildings during earthquakes in Turkey and Peru. Journal of Performance of Constructed Facilities. 2009;23(1):5-14. https://doi.org/10.1061/(asce)0887-3828(2009)23:1(5)

[2] Yılmaz S, Tama Y, Bilgin H. Seismic performance evaluation of unreinforced masonry school buildings in Turkey. Journal of Vibration and Control. 2013;19(16):2421-33. https://doi.org/10.1177/1077546312453190

[3] Bilgin H, Huta E. Earthquake performance assessment of low and mid-rise buildings: Emphasis on URM buildings in Albania. Earthquakes and Structures. 2018;14(6):599-614. https://doi.org/10.12989/eas.2018.14.6.599
[4] Estêvão J, Morales-Esteban A, Sá L, Ferreira M, Tomás B, Esteves C, et al. Improving the earthquake resilience of primary schools in the border regions of neighboring countries. Sustainability. 2022;14(23):15976. https://doi.org/10.3390/su142315976
[5] Bilgin H, Frangu I. Predicting the seismic performance of typical R/C healthcare facilities: emphasis on hospitals. International Journal of Advanced Structural Engineering. 2017;9:277-90. https://doi.org/10.1007/s40091-017-0164-y
[6] Organisation for Economic Co-operation and Development. Keeping schools safe in earthquakes. Proceedings of the Ad Hoc Experts' Group Meeting on Earthquake Safety in Schools; 2004 Feb 9-11; Paris, France. Paris: OECD; 2004.
[7] Bilgin H. Generation of fragility curves for typical RC health care facilities: Emphasis on hospitals in Turkey. Journal of Performance of Constructed Facilities. 2015;30(3):04015056. https://doi.org/10.1061/(ASCE)CF.1943-5509.0000806
[8] Bilgin H, Hysenlliu M. Comparison of near and far-fault ground motion effects on low and mid-rise masonry buildings. Journal of Building Engineering. 2020;30:101248. https://doi.org/10.1016/j.jobe.2020.101248
[9] Lagomarsino S, Penna A, Galasco A, Cattari S. TREMURI program: an equivalent frame model for the nonlinear seismic analysis of masonry buildings. Engineering Structures. 2013;56:1787-99. https://doi.org/10.1016/j.engstruct.2013.08.002
[10] KTP-N2-89. Albanian seismic design code. Tirana: Academy of Sciences; 1989. (In Albanian).
[11] NATO. SfP - 983054 Harmonization of seismic hazard maps for the Western Balkan countries (BSHAP). Final Report; 2010.
[12] Aliaj S, Kociu S, Muco B, Sulstarova E. Seismicity, seismotectonics and seismic hazard assessment in Albania. Tirana: Academy of Sciences of Albania; 2010.
[13] Istituto Nazionale di Geofisica e Vulcanologia. INGV shakemap archive [Internet]. 2019 [18 Feb 2020]. Available from: ingv.it
[14] U.S. Geological Survey. ANSS Comprehensive Earthquake Catalogue (ComCat) [Internet]. 2020 [20 Mar 2024]. Available from: usgs.gov
[15] Baytiyeh H. Why school resilience should be critical for the post-earthquake recovery of communities in divided societies. Education and Urban Society. 2017;51(5):693-711. https://doi.org/10.1177/0013124517747035
[16] Estêvão J, Ferreira M, Morales-Esteban A, Martínez-Álvarez F, Fazendeiro Sá L, Requena-García-Cruz MV. Earthquake resilient schools in Algarve (Portugal) and Huelva (Spain). In: 16th European Conference on Earthquake Engineering; 2018 Jun 18-21; Thessaloniki, Greece. 2018. str. 1–11.
[17] Alam M, Haque S. Seismic vulnerability evaluation of educational buildings of Mymensingh city, Bangladesh using rapid visual screening and index based approach. International Journal of Disaster Resilience in the Built Environment. 2020;11(3):379-402. https://doi.org/10.1108/ijdrbe-07-2019-0043
[18] Burton H, Deierlein G, Lallemant D, Lin T. Framework for incorporating probabilistic building performance in the assessment of community seismic resilience. Journal of Structural Engineering. 2016;142(8):C4015007. https://doi.org/10.1061/(asce)st.1943-541x.0001321
[19] Ausan R. Resiliency of a four-storey standard school building using the REDi framework. International Journal of Geomate. 2020;18(70):185-92. https://doi.org/10.21660/2020.70.9240
[20] Hejazi M, Jalaeefar A. Investigation of the seismic resilience of reinforced concrete special moment frames with infills. Structural Concrete. 2022;24(1):1083-101. https://doi.org/10.1002/suco.202100705
[21] Tabernero R, Ambrosini D, Curadelli O. Retrofitting of typical existing school buildings through seismic vulnerability assessment. Journal of Physics: Conference Series. 2024;2647(3):032005. https://doi.org/10.1088/1742-6596/2647/3/032005

[22] Rajarathnam S, Santhakumar A. Assessment of seismic building vulnerability based on rapid visual screening technique aided by aerial photographs on a GIS platform. Natural Hazards. 2015;78(2):779-802. https://doi.org/10.1007/s11069-014-1382-2
[23] Irvansyah R, Rusydy I, Simanjuntak A. A comparative analysis of seismic and tsunami fragility curves for school buildings in Banda Aceh coastal area. E3S Web of Conferences. 2022;340:02003. https://doi.org/10.1051/e3sconf/202234002003
[24] Marmolejos R, Germoso C, Omarbekova A. Local seismic response analysis based on the non-linear soil behavior: application to 5 essential buildings in Santiago de los Caballeros. In: 8th International Conference on Geotechnical and Earthquake Engineering (ICGRE 2023). https://doi.org/10.11159/icgre23.138
[25] González C, Niño M, Ayala G. Functionality loss and recovery time models for structural elements, non-structural components, and delay times to estimate the seismic resilience of Mexican school buildings. Buildings. 2023;13(6):1498. https://doi.org/10.3390/buildings13061498
[26] Athmani A, Grairia S, Seboui H, Khemis A, Formisano A, Ademović N. Integrated seismic vulnerability assessment for heritage educational buildings in Annaba city: combining probabilistic hazard analysis and structural modelling. Multidiscipline Modeling in Materials and Structures. 2024;20(6):1256-83. https://doi.org/10.1108/mmms-07-2024-0180
[27] Ribeiro F, Candeias P, Correia A, Carvalho A, Costa A. Risk and resilience assessment of Lisbon's school buildings based on seismic scenarios. Applied Sciences. 2022;12(17):8570. https://doi.org/10.3390/app12178570
[28] Liang L, Ohkubo T, Deng G, Cao J, Xu J. Reinforcement and effect evaluation of a middle school in Japan. Advances in Engineering Technology Research. 2024;10(1):103. https://doi.org/10.56028/aetr.10.1.103.2024
[29] Mucedero G, Perrone D, Monteiro R. Infill variability and modelling uncertainty implications on the seismic loss assessment of an existing RC Italian school building. Applied Sciences. 2022;12(23):12002. https://doi.org/10.3390/app122312002
[30] Gallo W, Clemett N, Gabbianelli G, O'Reilly G, Monteiro R. Seismic resilience assessment in optimally integrated retrofitting of existing school buildings in Italy. Buildings. 2022;12(6):845. https://doi.org/10.3390/buildings12060845
[31] Irvansyah R. Structural performance of Indonesian school building: a nonlinear static analysis for earthquake and tsunami loads. IOP Conference Series: Earth and Environmental Science. 2025;1479(1):012012. https://doi.org/10.1088/1755-1315/1479/1/012012
[32] Sharafi S, Saito T. Seismic damage probability assessment of existing reinforced concrete school buildings in Afghanistan. Buildings. 2024;14(4):1054. https://doi.org/10.3390/buildings14041054
[33] Zhou X, Xiang C. Seismic strengthening on masonry structure of primary and secondary school buildings. Applied Mechanics and Materials. 2011;71-78:626-30. https://doi.org/10.4028/www.scientific.net/amm.71-78.626
[34] Yong L, Zhang Y, Jing W, Xiong J. Research on the effective sheltering rates of public buildings in villages in western Sichuan, China—a case study of Ganbao Tibetan village. Buildings. 2024;14(7):2086. https://doi.org/10.3390/buildings14072086
[35] Wang Y, Peng D, Bo T, Zhao X, Bo J. A comprehensive evaluation method for assessing the seismic resilience of building sites based on the TOPSIS model and the entropy method. Buildings. 2024;14(11):3667. https://doi.org/10.3390/buildings14113667
[36] EN 1998-1. Eurocode 8: Design of structures for earthquake resistance - Part 1: General rules, seismic actions and rules for buildings. Brussels: European Committee for Standardization; 2004.
[37] TSDC. Building Earthquake Code of Turkey. Ankara: Disaster and Emergency Management Authority (AFAD); 2018.
[38] Xiao M, Xu H, Long X, Zhu J. Discussion on the method of pushover with cyclic loading. Advanced Materials Research. 2011;243-249:912-9. https://doi.org/10.4028/www.scientific.net/amr.243-249.912

[39] Skalomenos K, Papazafeiropoulos G. A computational method for performing nonlinear adaptive pushover analysis of structures through Abaqus simulation. In: 7th International Conference on Computational Methods in Structural Dynamics and Earthquake Engineering (COMPDYN 2019); 2019 Jun 24-26; Crete, Greece. 2019. str. 3955-64. https://doi.org/10.7712/120119.7199.19194
[40] Huang K, Kuang J. On the applicability of pushover analysis for seismic evaluation of medium- and high-rise buildings. The Structural Design of Tall and Special Buildings. 2010;19(5):573-88. https://doi.org/10.1002/tal.511
[41] Kovela P. Nonlinear pushover analysis for performance based engineering design – a review. International Journal for Research in Applied Science and Engineering Technology. 2017;5(3):1293-300. https://doi.org/10.22214/ijraset.2017.3239
[42] Bai J, Ou J. Seismic failure mode improvement of RC frame structure based on multiple lateral load patterns of pushover analyses. Science China Technological Sciences. 2011;54(11):2825-33. https://doi.org/10.1007/s11431-011-4469-y
[43] Lourenço P, Mendes N, Marques R. Earthquake design and assessment of masonry structures: review and applications. In: Topping BHV, Costa Neves LF, Barros RC, editors. Trends in Civil and Structural Engineering Computing. Stirlingshire: Saxe-Coburg Publications; 2009. Chapter 4. https://doi.org/10.4203/csets.22.4
[44] Maio R, Vicente R, Formisano A, Varum H. Seismic vulnerability of building aggregates through hybrid and indirect assessment techniques. Bulletin of Earthquake Engineering. 2015;13(10):2995-3014. https://doi.org/10.1007/s10518-015-9747-9
[45] Formisano A, Ademovic N. An overview on seismic analysis of masonry building aggregates. Frontiers in Built Environment. 2022;8:966281. https://doi.org/10.3389/fbuil.2022.966281
[46] Akhoundi F, Mohammadpour R, Shahbazi Y. Application of near surface mounted (NSM) technique for seismic retrofitting of heritage buildings. Journal of Research on Archaeometry. 2020;6(1):97-118. https://doi.org/10.29252/jra.6.1.97
[47] Chieffo N, Formisano A, Mochi G, Moșoarcă M. Seismic vulnerability assessment and simplified empirical formulation for predicting the vibration periods of structural units in aggregate configuration. Geosciences. 2021;11(7):287. https://doi.org/10.3390/geosciences11070287
[48] Vaiano G, Formisano A. Comparative analysis among different analysis programs for seismic vulnerability evaluation of a masonry building compound in the district of Naples. In: 8th International Conference on Computational Methods in Structural Dynamics and Earthquake Engineering (COMPDYN 2021); 2021 Jun 28-30; Athens, Greece. 2021. https://doi.org/10.7712/120121.8497.19272
[49] Formisano A, Chieffo N, Vaiano G. Seismic vulnerability assessment and strengthening interventions of structural units of a typical clustered masonry building in the Campania region of Italy. Geohazards. 2021;2(2):101-19. https://doi.org/10.3390/geohazards2020006
[50] Ademović N, Toholj M, Radonić D, Casarin F, Komesar S, Ugarković K. Post-earthquake assessment and strengthening of a cultural-heritage residential masonry building after the 2020 Zagreb earthquake. Buildings. 2022;12(11):2024. https://doi.org/10.3390/buildings12112024
[51] Pegoraro M, Saler E, Salvalaggio M, Valluzzi M. Modeling strategies for non-linear seismic analyses: comparison among EFM and FEM results on an existing URM case study. In: 8th International Conference on Computational Methods in Structural Dynamics and Earthquake Engineering (COMPDYN 2021); 2021 Jun 28-30; Athens, Greece. 2021. https://doi.org/10.7712/120121.8479.18857